

Characteristic Behavior of Carbon Nanotubes

— Kinematics of Persistent Currents —

K. Sasaki and Y. Kawazoe

Institute for Materials Research, Tohoku University, Sendai 980-8577, Japan

The electrical properties of a carbon nanotube depend strongly on its lattice structure as defined by chiral and translational vectors. A toroidal shape for a nanotube allows various twisted structures to occur in the direction of the tube axis. We investigate theoretically the kinematics of conducting electrons and persistent currents in toroidal carbon nanotubes. We show that persistent currents exhibit a special characteristic of the cylindrical lattice structure for twisted cases. We discuss the possibilities that the twist alters the period of the current to one half the flux quantum, and that the current flows without an external magnetic field.

§1. Introduction

Carbon nanotubes¹⁾ (CNTs) are cylindrical molecules with a diameter as small as one nanometer and a length up to several micrometers. They consist of carbon atoms only and can be thought of as a graphene sheet wrapped into a cylinder. They exhibit either metallic or semiconducting behavior depending on the diameter and chirality of the hexagonal carbon lattice of the tube.²⁾⁻⁴⁾ It is quite important to understand the electrical properties of the carbon nanotube which are governed mainly by low-energy electrons near the Fermi level. Thus far theoretical research has been done on the low-energy electrical properties of metallic nanotubes. Because a nanotube is very long and thin, theorists analyze its properties by regarding it as a one-dimensional object. These analyses, based on the method developed by Tomonaga and Luttinger (TL-liquid theory), reveal the nature of the correlated system and experimentally observe the characteristic feature of the correlation as a power-law dependence of resistivity on temperature.^{5),6)} Taking into account the successful application of TL-liquid theory to CNTs, in terms of their low-energy electrical behavior CNT systems seem very similar to conventional one-dimensional material such as a chain of atoms. Accordingly, the following question naturally arises: “How does a nanotube differ from conventional one-dimensional material, such as a chain of atoms?” In this respect, we note the persistent currents in toroidal carbon nanotubes⁷⁾ (torus geometry, a tube curved so that both ends connect, is hereafter referred to as “torus” or “nanotorus” for simplicity).

Persistent currents in mesoscopic rings are known phenomena in condensed matter physics.⁸⁾⁻¹⁰⁾ Conservation of the electron phase coherence in a whole sample can affect the equilibrium properties of the system. One of the most striking consequences of this is that a single isolated mesoscopic normal-metal ring threaded by a magnetic flux is thought to carry a (persistent) current, in the form of a sawtooth curve with period Φ_0 , the single-electron flux quantum. In this paper, we show that

nanotori can exhibit special persistent currents not seen in the usual mesoscopic systems. For example, some types of nanotori exhibit a sawtooth curve with a period one half the flux quantum. We point this out as an effect reflecting the geometrical structure of the (graphite) cylinder, that is, conducting electrons have a new degree of freedom to rotate around the tubule axis that is not found in conventional one-dimensional material such as a chain of atoms.

Here, we would like to mention the relationship between our work and previously published literature on persistent currents in carbon nanotori. Lin and Chuu¹¹⁾ performed numerical estimations of persistent currents in untwisted nanotori and found structure dependent currents. Later, a non-trivial geometrical degree of *twist*¹²⁾ was taken into account by Margańska and Szopa.¹¹⁾ From a numerical calculation, they concluded that for a specific type of twisted torus, the twist has no significant influence on persistent current. The above-mentioned authors employed a simple nearest-neighbor tight-binding Hamiltonian that was shown to be good approximation for describing the conducting electrons in nanotubes.²⁾ In this paper, we use the same Hamiltonian and examine persistent currents in all possible types of torus geometry analytically and consider the possibility that carbon nanotori exhibit unusual (and new) phenomena. We clarify two interesting possibilities: (1) the twist can change the period of the current to one half the flux quantum, and (2) current may flow without an external magnetic field. One can include various effects on persistent currents in the analysis. The curvature effect was analyzed by Lin et al.,¹³⁾ and the effect of disorder on persistent currents was taken into account by Latil et al.¹³⁾ as position-dependent on-site energy. The effect of Coulomb interactions was examined by Odintsov et al.¹³⁾ and Sasaki.¹³⁾ Liu et al.⁷⁾ observed toroidal structures experimentally. On the other hand, Martel et al. and Ahlskog et al.¹⁴⁾ suggested that they were likely to be coiled nanotubes stabilized by van der Waals interactions.

This paper is organized as follows. In Sections 2 and 3, we review the basis for the kinematics of conducting electrons in untwisted nanotori and the persistent currents in those systems. We examine persistent currents not only in metallic structures but also in semiconducting chiral structures assuming that a finite number of states exist near the Fermi level. (While this is true for metallic nanotori, it is not true for half-filled semiconducting nanotori. However, given that a sufficient number of electrons are added into the system, it is possible to observe the persistent current.) In Sections 4 and 5, we clarify the kinematics of electrons in twisted nanotori and examine the persistent currents. We study the effects of the twist on persistent currents and show that, due to the cylindrical lattice structure of the nanotube, a special current can flow in these systems. In Section 6 we summarize and discuss our results, and in Section 7 we give our conclusions. For the purposes of this study, we work in units of $\hbar = c = 1$.

§2. Kinematics of an untwisted torus

We begin by specifying the lattice structure of a nanotorus. A nanotorus is regarded as a nanotube with the ends connected together. The nanotube is a graphene

sheet wrapped to form a cylinder. Thus, a nanotorus is classified by its chiral and translational vectors defined respectively by

$$C_h = nT_1 + mT_2, \quad T = pT_1 + qT_2, \quad (1)$$

where T_1 and T_2 are symmetry translation vectors on the planar honeycomb lattice ^{*)}. The two sets of integers (n, m) and (p, q) specify the lattice structure around and along the axis, respectively. Notice that, in the case of a torus, the chiral vector does not determine the translational vector as contrasted with nanotubes where integers (n, m) completely fix a unit of the translational vector: $(p, q)/\text{gcd}(p, q)$.²⁾ Here, $\text{gcd}(p, q)$ denotes the greatest common divisor of the two integers p and q .

We define for the *untwisted* torus chiral and translational vectors which satisfy

$$C_h \cdot T = 0. \quad (2)$$

This condition ensures the absence of *twist* along the axis so that $(p, q)/\text{gcd}(p, q)$ is determined by the chiral vector only. An untwisted torus can be unrolled to a rectangular graphene sheet as is shown in Fig. 1. We classify nanotori for which the translational vector does not satisfy Eq. (2) as a *twisted* torus, which we will investigate in later sections of this paper. Making use of Eqs. (1) and (2), we can rewrite (p, q) for an untwisted torus as

$$\frac{p}{d_T} = \frac{2m+n}{d_R}, \quad \frac{q}{d_T} = -\frac{2n+m}{d_R}, \quad (3)$$

where $d_R \equiv \text{gcd}(2m+n, 2n+m)$ and $d_T \equiv \text{gcd}(p, q)$. By introducing $d \equiv \text{gcd}(n, m)$, one obtains $d_R = \text{gcd}(3d, n-m)$, a useful identity for classifying the lattice structures of nanotubes²⁾ and also for understanding persistent currents in nanotori.

The quantum mechanical states of the conducting electrons (π -electrons) are labeled by the wave vectors. The wave vector is fixed by the lattice structure of the nanotorus through the boundary conditions. We define unit wave vectors k_{\perp} and k_{\parallel} for an untwisted torus by the periodic boundary conditions

$$C_h \cdot k_{\perp} = 2\pi, \quad C_h \cdot k_{\parallel} = 0, \quad T \cdot k_{\perp} = 0, \quad T \cdot k_{\parallel} = 2\pi. \quad (4)$$

Here, k_{\perp} and k_{\parallel} are expressed in terms of the reciprocal lattice vectors (K_1 and K_2) as

$$k_{\perp} = \frac{1}{N_c}(-qK_1 + pK_2), \quad k_{\parallel} = \frac{1}{N_c}(mK_1 - nK_2), \quad (5)$$

where $N_c \equiv mp - nq$, and we have defined the reciprocal lattice vectors of the graphene sheet by $K_i \cdot T_j = 2\pi\delta_{ij}$ ($i, j = 1, 2$). It should be noted that $|N_c|$ corresponds to the total number of hexagons in an untwisted nanotorus because of

^{*)} A schematic diagram of the honeycomb lattice and the notation used in this paper can be found in Ref. 13) (Sasaki). The symmetry translation vectors can be expressed as $T_1 = \sqrt{3}ae_x$, $T_2 = (\sqrt{3}/2)ae_x + (3/2)ae_y$, where a denotes the length between two nearest carbon sites, and each site is linked by the vectors u_a ($a = 1, 2, 3$). They are given explicitly by $u_1 = ae_y$, $u_2 = -(\sqrt{3}/2)ae_x - (1/2)ae_y$, $u_3 = (\sqrt{3}/2)ae_x - (1/2)ae_y$.

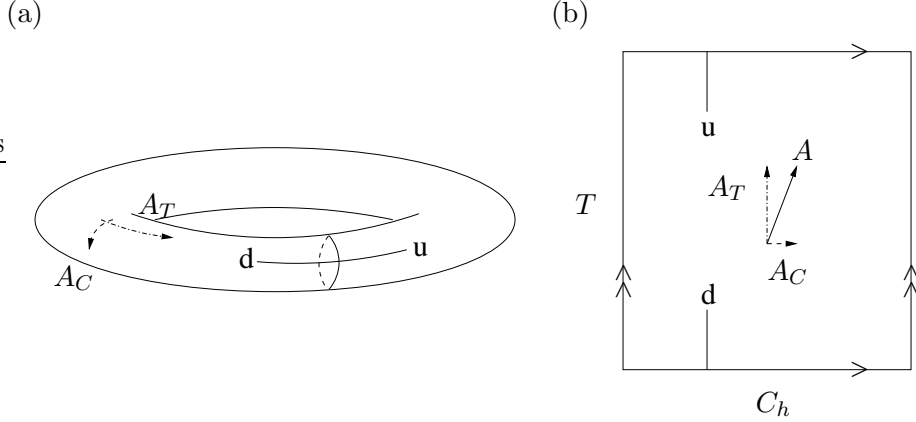


Fig. 1. Schematic diagram of an untwisted torus (a) and its net (b) with an external gauge field. The two lines extending upward from ‘u’ and downward from ‘d’ are joined to form an untwisted torus.

$C_h \times T = N_c(T_1 \times T_2)$ and is an even number. We decompose wave vector k as $\mu_\perp k_\perp + \mu_\parallel k_\parallel$ where μ_\perp and μ_\parallel are integers satisfying the Brillouin zone:

$$\left[-\frac{d}{2} \right] + 1 \leq \mu_\perp \leq \left[\frac{d}{2} \right], \quad \left[-\frac{N_c}{2d} \right] + 1 \leq \mu_\parallel \leq \left[\frac{N_c}{2d} \right]. \quad (6)$$

It should also be noted that the wave vectors, which can be *congruent* to each other, can be identified with the same state. Mathematically, wave vectors k and $k + \delta k$ are equivalent if δk can be written as

$$\delta k \equiv \delta \mu_\perp k_\perp + \delta \mu_\parallel k_\parallel = \tau_1 K_1 + \tau_2 K_2, \quad (7)$$

where τ_1 and τ_2 are integers. It follows from Eqs. (5) and (7) that

$$\delta \mu_\perp = n \tau_1 + m \tau_2, \quad \delta \mu_\parallel = p \tau_1 + q \tau_2. \quad (8)$$

Using this degree of freedom, one may change the first term of Eq.(6) to $0 \leq \mu_\perp \leq d - 1$. Nevertheless, we will use Eq.(6) because the wave vector $\mu_\perp k_\perp$ implies the momentum around the axis, which should be positive and negative (or zero). The rotating motion of the electron around the axis is expressed by a negative μ_\perp for the clockwise direction and a positive μ_\perp for the counterclockwise direction, which is manifest in Eq.(6).

§3. Persistent currents in an untwisted torus

In this section, we consider persistent currents in untwisted nanotori. We suppose that the Hamiltonian for the π -electrons in an external gauge field A is given by the nearest-neighbor tight-binding Hamiltonian:

$$\mathcal{H} = V_\pi \sum_{\langle i,j \rangle} a_j^\dagger e^{-ie \int_{r_i}^{r_j} A \cdot ds} a_i, \quad (9)$$

where V_π is the hopping integral, and sum $\langle i, j \rangle$ is over pairs of nearest-neighbor carbon sites i, j on the surface. Vector r_i labels the vector pointing toward each site i , and a_i and a_i^\dagger are canonical annihilation-creation operators of the site i electron that satisfy the anti-commutation relation $\{a_i, a_j^\dagger\} = \delta_{ij}$. Finally, $-e$ is the electron charge and ds is the differential line element on the surface. Generally, the gauge field has two components: $A \cdot T = A_T$ and $A \cdot C_h = A_C$. A_T can be controlled by the Aharonov-Bohm flux penetrating the ring and A_C corresponds to the magnetic flux within the surface of a nanotorus (see Fig. 1).

We diagonalize the Hamiltonian using the Bloch base states and obtain the energy eigenvalue:

$$E(k - eA) = -V_\pi \left| \sum_{a=1,2,3} e^{i(k - eA) \cdot u_a} \right|, \quad (10)$$

where $E(k - eA)$ denotes the energy eigenvalue below the Fermi level ($E \leq 0$). Here, vector u_a ($a = 1, 2, 3$) is a triad of vectors pointing, respectively, in the direction of the nearest neighbors of a carbon site. For non-interacting theories, the persistent current can be calculated by the behavior of electrons near the Fermi level.¹⁰⁾ It is therefore convenient to select energy bands for which the electronic states are located closest to the Fermi level. Hereafter, we will call those energy bands *low energy bands*. By studying the energy dispersion relation of the Hamiltonian, we can see that there are two independent Fermi points. They are placed at

$$\pm K + \tau_1 K_1 + \tau_2 K_2, \quad (11)$$

where $K \equiv (2K_1 + K_2)/3$ satisfies $E(\pm K) = 0$, and (τ_1, τ_2) is a set of integers indicating the congruent degree of freedom. It is easy to find the index μ_\perp of the low energy bands. We denote them as $\pm \mu_\perp^0$, which is given by

$$\mu_\perp^0 = \left\langle \frac{2n + m}{3} \right\rangle + n\tau_1 + m\tau_2. \quad (12)$$

Here, $\langle a \rangle$ means the closest integer to the number a , that is, a rounded. In the following consideration, it is important to verify that the electrons in the low energy bands are *rotating* around the axis. In other words, it is crucial to determine if the wave function of electrons in the low energy bands is a constant around the axis (see Fig. 2). One may regard the electrons in the low energy band as *non-rotating* if μ_\perp^0 can be congruent to zero by an appropriate choice of τ_1 and τ_2 . The condition of non-rotating mode is therefore

$$\exists(\tau_1, \tau_2) \in \mathbb{Z} \cdot \mu_\perp^0 = 0. \quad (13)$$

In Table I, we list several types of chiral structures and determine if the electrons in the low energy bands are rotating. The left index in Table I indicates the chirality where $(n, 0)$ is zigzag, (n, n) is armchair and the others are classified by chiral type.

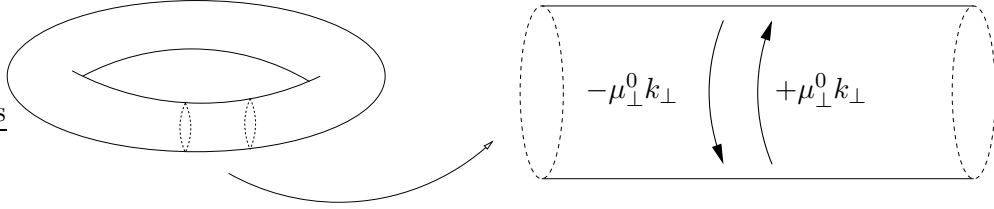


Fig. 2. A part of a nanotorus in which the motion of electrons near the Fermi level are shown (axial motion is neglected). The arrows show two modes near the Fermi level, or the motion of electrons in the low energy bands. If μ_\perp^0 can be congruent to zero, there is no rotational motion around the axis. In this case, the wave function of the electrons can be regarded as a constant around the axis.

Chirality	Index of Low Energy Bands	“Rotating?”
$C_h = (n, m)$	$\mu_\perp^0 = \langle \frac{2n+m}{3} \rangle + n\tau_1 + m\tau_2$	$\mu_\perp^0 \not\equiv 0 ?$
$(n, 0)$ zigzag	$\langle \frac{2n}{3} \rangle + n\tau_1$	Yes if $(n \neq 1)$
(n, n) armchair	$n + n\tau_1 + n\tau_2$	No
$(n, 2n)$ chiral	$\langle \frac{4n}{3} \rangle + n\tau_1 + 2n\tau_2$	Yes if $(n \neq 1)$
$(n, 3n)$ chiral	$\langle \frac{5n}{3} \rangle + n\tau_1 + 3n\tau_2$	Yes if $(n \neq 1)$
$(n, 4n)$ chiral	$2n + n\tau_1 + 4n\tau_2$	No

Table I. Untwisted nanotori and electron motion in the low energy bands.

The low energy bands are classified as rotating state or non-rotating state depending on μ_\perp^0 in the center and right indices. It is noted that when $d = 1$, such as a $(7, 4)$ chiral nanotube, μ_\perp^0 is always congruent to zero because $6 + 7\tau_1 + 4\tau_2 = 0$ holds for $(\tau_1, \tau_2) = (6, -12)$.

Proceeding now to the lattice structure along the axis, we examine the wave vector of the electron located nearest to the Fermi points in the low energy bands. After calculating, we obtain the condition for choosing the state. We label the wave vector along the axis of that state by μ_\parallel^0 and it satisfies

$$\left\langle \mu_\parallel^0 \frac{d_R}{d_T} \right\rangle = m. \quad (14)$$

Depending on $\mu_\parallel^0 d_R / d_T$, we divide the axial structures into two classes as follows

$$\begin{cases} \mu_\parallel^0 \frac{d_R}{d_T} = m : \text{m-class,} \\ \mu_\parallel^0 \frac{d_R}{d_T} \neq m : \text{s-class.} \end{cases} \quad (15)$$

Now, we consider d_R for the two cases $d_R = d$ and $d_R = 3d$.²⁾ When $d_R = d$, because m/d is always an integer, we can choose an integer $\mu_\parallel^0 = d_T(m/d)$ that satisfies the condition for m-class. On the other hand, when $d_R = 3d$, if d_T is a multiple of

3 this also qualifies as m-class while all the other cases are considered s-class. To summarize our classification, then,

$$d_R = d : \text{m-class}, \quad (16)$$

$$d_R = 3d : \begin{cases} d_T = 3a : & \text{m-class,} \\ d_T = 3a + i \ (i = 1, 2) : & \text{s-class.} \end{cases} \quad (17)$$

where a is an integer. For m-class, the persistent current is the standard one. That is, the persistent current does not differ from the standard sawtooth curve with a period equal to the flux quantum. However, for s-class, the electron near one of the Fermi points touches the Fermi level when $\Phi_0/3$ flux is turned on, and the other electron near another Fermi point goes to the Fermi level when $-\Phi_0/3$ flux pierces the torus. Therefore, the resultant current is given by a superposition of two sawtooth curves whose origins (or zero amplitude positions) are shifted in different directions by $\pm\Phi_0/3$. This phenomenon was observed numerically by Lin and Chuu¹¹⁾ and is a consequence of the well-known fact that one third of zigzag nanotubes are metallic and the other two-thirds of zigzag nanotubes are semiconducting.

§4. Kinematics of a twisted torus

In the previous sections we examined the kinematics and persistent currents in untwisted nanotori. Here, the twisted torus is investigated. We define the translational vector for a twisted torus as T_w that satisfies $C_h \cdot T_w \neq 0$. All lattice structures except the untwisted torus belong to the twisted nanotorus (see Fig. 3). Among the various lattice structures of the twisted torus, we first examine a type that can be obtained from an untwisted nanotorus. For this type, we can assign an untwisted torus having a translational vector that satisfies

$$T_w - T \parallel C_h, \quad (18)$$

where T is the translational vector of the corresponding untwisted nanotorus. We call this an “A-type” twisted nanotorus. We will refer to another type of twisted nanotorus as “B-type” for which we can also assign an untwisted nanotorus. It is defined in such a way that $|T_w - T|$ becomes minimum length. As an example of a B-type twisted nanotorus, we take the chiral vector as zigzag $(n, 0)$, and the translation vector as $(d_t, -2d_t + 1)$, where d_t is an integer. The nanotorus is twisted because $C_h \cdot T_w = nT_1 \cdot T_2 \neq 0$. Defining the corresponding untwisted torus for this twisted torus as $T = d_t T_1 - 2d_t T_2$, we then have $T_w - T = T_2$, which is not parallel to $C_h (= nT_1)$. We limit ourselves to a study of the A-type nanotorus in this section. We will examine B-type nanotori in a subsequent section.

We set the chiral and translational vectors of an A-type twisted nanotorus to $C_h = nT_1 + mT_2$ and $T_w = pT_1 + qT_2$, respectively, for a corresponding untwisted torus of $T = \bar{p}T_1 + \bar{q}T_2$. By Eq.(18), we can relate (p, q) to (\bar{p}, \bar{q}) using (n, m) and an integer t as

$$p = \bar{p} + t \frac{n}{d}, \quad q = \bar{q} + t \frac{m}{d}. \quad (19)$$

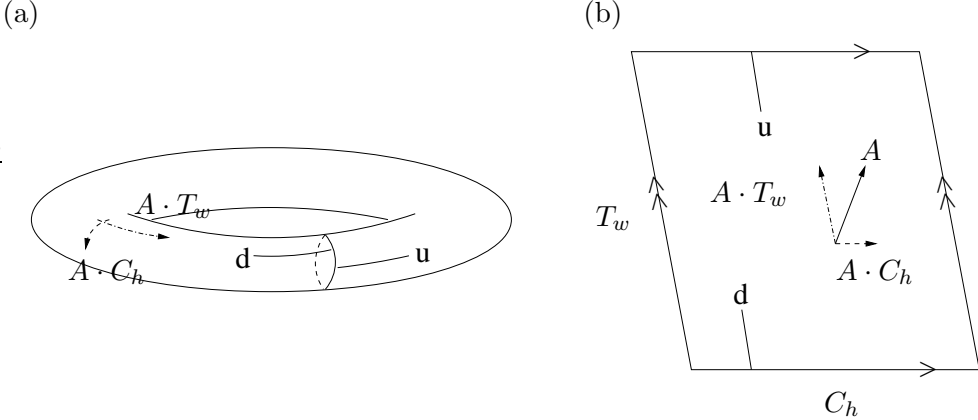


Fig. 3. Schematic diagram of a twisted torus (a) and its net (b) with an external gauge field. It is convenient to consider a parallelogram as the net of a twisted torus. Note that the two lines, extending upward from ‘u’ and downward from ‘d’ are not joined contrary to the untwisted case.

Integer t determines the amount of twist, and in the case of a vanishing t a twisted torus becomes an untwisted one.

To study the Hilbert space of conducting electrons in a twisted nanotorus, we decompose wave vector k as $\mu_1 k_1 + \mu_2 k_2$ where unit wave vectors k_1 and k_2 are defined as

$$C_h \cdot k_1 = 2\pi, \quad C_h \cdot k_2 = 0, \quad T_w \cdot k_1 = 0, \quad T_w \cdot k_2 = 2\pi. \quad (20)$$

The unit vectors are rewritten in terms of the reciprocal lattice vectors as

$$k_1 = \frac{1}{N_c}(-qK_1 + pK_2), \quad k_2 = \frac{1}{N_c}(mK_1 - nK_2), \quad (21)$$

Note that for an A-type torus, N_c is still an even number and is the same as that of the corresponding untwisted nanotorus ($N_c = mp - nq = m\bar{p} - n\bar{q}$). As in the case of the untwisted nanotorus, μ_1 and μ_2 have the following congruent degree of freedom: $\delta\mu_1 = n\tau_1 + m\tau_2$ and $\delta\mu_2 = p\tau_1 + q\tau_2$ where τ_1 and τ_2 are integers.

§5. Persistent currents in a twisted torus

In this section, we examine persistent currents in twisted nanotori. A primary conclusion is that persistent currents change according to the degree of twist from untwisted. The change depends crucially on the following two factors: (1) whether or not there is a periodic lattice structure around the axis, that is, whether $d \geq 2$ or $d = 1$, respectively, and (2) whether or not electrons near the Fermi level are rotating around the axis. This rotational degree of freedom is a new characteristic that conventional one-dimensional material (such as a chain of atoms) does not possess.

We start by specifying the low energy bands in twisted nanotori. Even with twisted nanotori, the index of the low energy bands is determined by the same conditions as for the untwisted torus (Eq.13). We set the energy band index as μ_1^0

for a condition of non-rotating state given by,

$$\exists(\tau_1, \tau_2) \in Z \cdot \mu_1^0 = \left\langle \frac{2n+m}{3} \right\rangle + n\tau_1 + m\tau_2 = 0. \quad (22)$$

There are two low energy bands for which the wave vectors around the axis are given by $\pm\mu_1^0 k_1$. To examine the persistent currents, we consider the energy dispersion relationship of the low energy bands:

$$E_{\pm} = -V_{\pi} \left| \sum_{a=1,2,3} z_{a\pm} \right| = -V_{\pi} (3 + 2\Re [z_{1\pm}^* z_{2\pm} + z_{1\pm}^* z_{3\pm} + z_{2\pm}^* z_{3\pm}]), \quad (23)$$

where we have defined

$$z_{a\pm} \equiv \exp (i(\pm\mu_1^0 k_1 + \mu_2 k_2 - eA) \cdot u_a). \quad (24)$$

It is not necessary to estimate the numerical value of E_{\pm} to understand what is happening in twisted nanotori. It is enough to understand the difference between persistent currents in untwisted and twisted tori. For this purpose, it is convenient to rewrite vector u_a in terms of the chiral and translational vectors as

$$\begin{aligned} u_1 &= \frac{2}{3N_c} \left[\left(p + \frac{q}{2} \right) C_h - \left(n + \frac{m}{2} \right) T_w \right], \\ u_2 &= \frac{2}{3N_c} \left[-\left(\frac{p-q}{2} \right) C_h + \left(\frac{n-m}{2} \right) T_w \right], \\ u_3 &= \frac{2}{3N_c} \left[-\left(\frac{p}{2} + q \right) C_h + \left(\frac{n}{2} + m \right) T_w \right]. \end{aligned} \quad (25)$$

In the absence of an external magnetic flux within the surface of the nanotorus, we can set the gauge as $A \cdot C_h = 0$. Substituting Eq.(25) into Eq.(24) and using Eq.(20), we obtain

$$\begin{aligned} z_{1\pm}^* z_{2\pm} &= e^{-i(\pm 2\pi\mu_1^0) \frac{p}{N_c}} e^{i(2\pi\mu_2 - eA \cdot T_w) \frac{n}{N_c}}, \\ z_{1\pm}^* z_{3\pm} &= e^{-i(\pm 2\pi\mu_1^0) \frac{p+q}{N_c}} e^{i(2\pi\mu_2 - eA \cdot T_w) \frac{n+m}{N_c}}, \\ z_{2\pm}^* z_{3\pm} &= e^{-i(\pm 2\pi\mu_1^0) \frac{q}{N_c}} e^{i(2\pi\mu_2 - eA \cdot T_w) \frac{m}{N_c}}. \end{aligned} \quad (26)$$

For an A-type twisted nanotorus, we can further rewrite the above equations using Eq.(19) as

$$\begin{aligned} z_{1\pm}^* z_{2\pm} &= e^{-i(\pm 2\pi\mu_1^0) \frac{\bar{p}}{N_c}} e^{i(2\pi\mu_2 - eA \cdot T_w \mp 2\pi\mu_1^0 \frac{t}{d}) \frac{n}{N_c}}, \\ z_{1\pm}^* z_{3\pm} &= e^{-i(\pm 2\pi\mu_1^0) \frac{\bar{p}+\bar{q}}{N_c}} e^{i(2\pi\mu_2 - eA \cdot T_w \mp 2\pi\mu_1^0 \frac{t}{d}) \frac{n+m}{N_c}}, \\ z_{2\pm}^* z_{3\pm} &= e^{-i(\pm 2\pi\mu_1^0) \frac{\bar{q}}{N_c}} e^{i(2\pi\mu_2 - eA \cdot T_w \mp 2\pi\mu_1^0 \frac{t}{d}) \frac{m}{N_c}}. \end{aligned} \quad (27)$$

Comparing this with the wave vector in an untwisted nanotorus ($t = 0$ case), we observe that the twist produces a shift of the wave vector along the axis. This effect

can be regarded as a kind of gauge field induced by the twist,¹⁵⁾ assuming that the sign of electron *charge* depends on the direction of *rotation* around the axis. The twist induces gauge field A^{twist} . Electron in the low energy bands having charge (e_{\pm}) couple to A^{twist} then feel the effect of the total gauge field as $A \rightarrow A + A^{\text{twist}}$ where

$$eA \cdot T_w = 2\pi \frac{\Phi}{\Phi_0}, \quad e_{\pm} A^{\text{twist}} \cdot T_w \equiv \pm 2\pi \mu_1^0 \frac{t}{d}. \quad (28)$$

Here, Φ is the Aharonov-Bohm flux piercing the twisted torus.

Let us verify the above result for an A-type twisted zigzag nanotorus for which the chiral and translational vectors are defined by $(n, 0)$ and (p, q) where $p = \bar{p} + n_t$ and $q = \bar{q}$. Constant n_t expresses the number of hexagons twisted at the junction (see Fig. 3(a)). In this case, we have

$$e_{\pm} A^{\text{twist}} \cdot T_w = \pm 2\pi \mu_1^0 \frac{n_t}{n}. \quad (29)$$

Hence, for the $(9, 0)$ chiral vector, because $\mu_1^0 = 6$, we obtain a $\pm \frac{4\pi}{3} n_t$ shift in the persistent current. We can imagine that $\frac{2}{3} n_t \Phi_0$ magnetic flux penetrates the ring on the assumption that electrons in the low energy bands have a charge of opposite sign depending on the direction of rotation around the axis, that is, clockwise (+) and counterclockwise (-) or vice versa (see Fig. 4). On the other hand, for an armchair chiral structure, the low energy band is always classified as the non-rotating state, i.e., μ_1^0 can be regarded as zero (see Table I). As a result, the twist does not affect the persistent current. In other words, electrons near the Fermi level have vanishing charge couples to A^{twist} .

We consider some possible consequences of the twist-induced gauge field. First, it is valuable to assume that the period of the persistent current becomes one half the flux quantum. Conventional one-dimensional material exhibits a period equal to the flux quantum, except for the case of the superconducting state where a sawtooth curve with a period of one half the flux quantum is expected. Due to its twisted lattice structure, a carbon nanotorus allows a persistent current, with a period one half the flux quantum even though the electrons do not develop the superconducting state. The condition for a period of one half is given by

$$e_{\pm} A^{\text{twist}} \cdot T_w = \pm \frac{\pi}{2} + 2\pi i \leftrightarrow \mu_1^0 \frac{t}{d} = \pm \frac{1}{4} + i, \quad (30)$$

where i is an integer. It should be mentioned that the phenomena of the half period may also be realized in an untwisted torus when the two low energy bands have even and odd (or odd and even) numbers of electrons ^{*)}. However, in the case of the twisted nanotorus, the additional surprising phenomenon of a vanishing external magnetic field can be expected. Let us consider an m-class untwisted torus and suppose that the number of electrons is even in the $+\mu_1^0$ energy band and odd in

^{*)} The one-half periodicity might be realized even in a conventional one-dimensional material when we assume even-odd asymmetry for spin up-down conducting electrons. Note also that the one-half period phenomena were experimentally observed in systems of a large number of loops and believed to be due to their ensemble average.⁹⁾

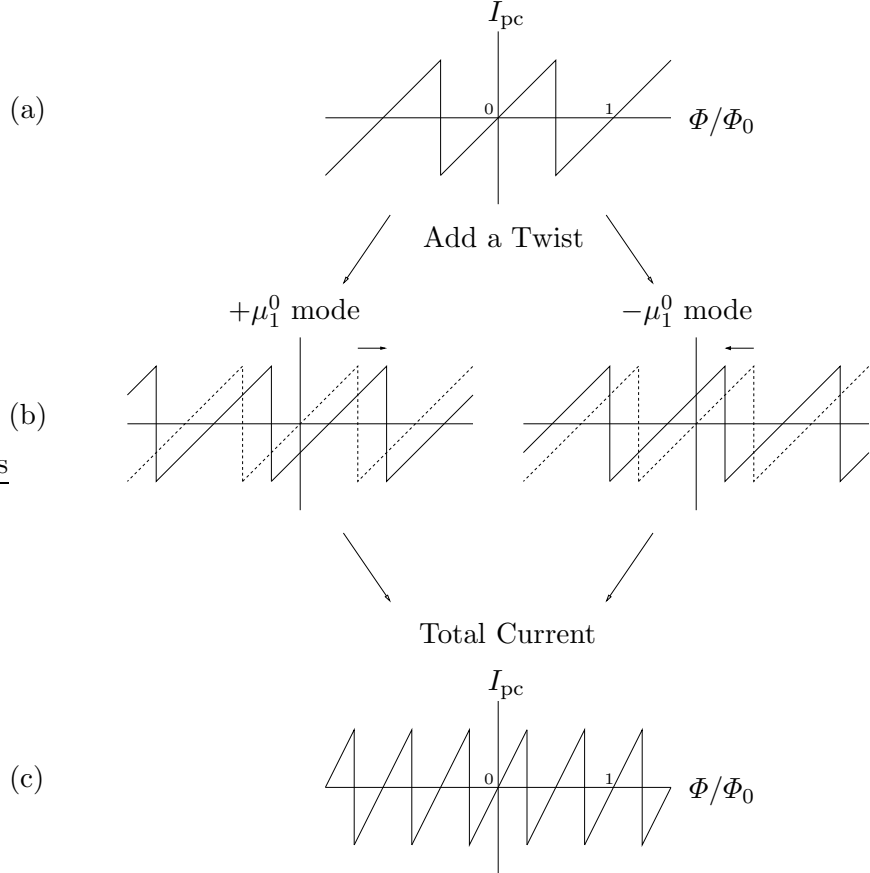


Fig. 4. (a) Sawtooth curve of a persistent current (I_{pc}) in an untwisted (m-class) torus as a function of magnetic flux. The period of the curve is given by the flux quantum Φ_0 . (b) The twist shifts the curves in the positive and negative directions depending on the electrons' motion around the axis: clockwise and counterclockwise directions. The total persistent current is given by the sum of two currents. As an example, we depict the case of Eq.(30) in (c).

the $-\mu_1^0$ energy band. The zero amplitude positions of the persistent currents are different from each other, or the phases differ from each other by π , so that we have the one-half periodicity. Then, by twisting the untwisted nanotorus, the persistent currents of both modes shift in different directions and the amplitude of the total current has a chance to be a finite value. In this case, the persistent current can flow in the twisted torus with no external magnetic field.

We now examine the case of B-type twisted nanotori. We set the translation vector for a B-type twisted torus as (p, q) and the corresponding untwisted torus as (\bar{p}, \bar{q}) and relate them as $p = \bar{p} + \delta p$ and $q = \bar{q} + \delta q$. After calculating, we get

$$\begin{aligned}
 z_{1\pm}^* z_{2\pm} &= e^{-i\frac{2\pi}{N_c} \left(\pm \mu_1^0 p - \frac{eA \cdot C_h}{2\pi} \bar{p} - \mu_2 n + \frac{eA \cdot T_w}{2\pi} n \right)}, \\
 z_{1\pm}^* z_{3\pm} &= e^{-i\frac{2\pi}{N_c} \left(\pm \mu_1^0 (p+q) - \frac{eA \cdot C_h}{2\pi} (\bar{p}+\bar{q}) - \mu_2 (n+m) + \frac{eA \cdot T_w}{2\pi} (n+m) \right)}, \tag{31}
 \end{aligned}$$

$$z_{2\pm}^* z_{3\pm} = e^{-i\frac{2\pi}{N_c} \left(\pm \mu_1^0 q - \frac{eA \cdot C_h}{2\pi} \bar{q} - \mu_2 m + \frac{eA \cdot T_w}{2\pi} m \right)}.$$

Proceeding further, we set $\delta p T_1 + \delta q T_2 = \alpha C_h + \beta T$ where (α, β) are fractions. Note that, $\beta = 0$ ($\beta \neq 0$) indicates for an A-type (B-type) twisted nanotorus. Using this definition, we obtain $\delta p = \alpha n + \beta \bar{p}$ and $\delta q = \alpha m + \beta \bar{q}$. It is clear that the effect of β -term can be absorbed into the effective gauge field as before, but this time the inner product of A^{twist} and the chiral vector does not vanish:

$$e_{\pm} A^{\text{twist}} \cdot T_w \equiv \pm 2\pi \mu_1^0 \alpha, \quad e_{\pm} A^{\text{twist}} \cdot C_h \equiv \pm 2\pi \mu_1^0 \beta. \quad (32)$$

Note that $|\beta| \ll |\alpha|$ holds for lattice structures satisfying $|T_w - T| \leq |C_h|$ and $|T| \gg |C_h|$. The effect of the β term on the electrical properties will become important when we consider a small $|T| \sim \mathcal{O}(|C_h|)$ nanotorus. This result indicates that a B-type twisted nanotorus may have a tiny energy gap even if its corresponding untwisted torus is classified as a metallic system and m-class.

We now present a simple derivation of the final result of Eq.(32). For both twisted and untwisted tori, we have defined the unit wave vectors as given in Eqs.(5) and (21). They are related to each other by

$$k_1 = \frac{\bar{N}_c}{N_c} k_{\perp} + \frac{1}{N_c} (-\delta q K_1 + \delta p K_2), \quad k_2 = \frac{\bar{N}_c}{N_c} k_{\parallel}, \quad (33)$$

where $N_c = mp - nq$ and $\bar{N}_c \equiv m\bar{p} - n\bar{q}$. It is noted that $N_c = \bar{N}_c$ holds for A-type twisted nanotori, however, no such relation can be expected for the B-type torus. The key physical quantity is shown at the right hand side of the first equation, where

$$\begin{aligned} \frac{1}{N_c} (-\delta q K_1 + \delta p K_2) &= \frac{1}{N_c} [(-n\delta q + m\delta p) k_{\perp} + (-\bar{p}\delta q + \bar{q}\delta p) k_{\parallel}] \\ &= \frac{\bar{N}_c}{N_c} [\beta k_{\perp} - \alpha k_{\parallel}]. \end{aligned} \quad (34)$$

The above equation indicates that the wave vectors around and along the axis change according to the twist β and α . These terms can be thought of as an effective gauge field due to the gauge coupling, and this is why persistent currents exhibit a distinctive shape.

§6. Summary and Discussion

We have studied the kinematics of π -electrons in nanotori and have shown that persistent currents depend on the lattice structure. In particular, we have clarified the effects of twist on persistent currents and revealed two consequences: the flux period can be one half of the single-electron flux quantum, and non-vanishing current can flow without an external magnetic field. We have shown that in order to observe the effect of twist on persistent currents, the following geometrical conditions have to be satisfied: (1) there must be a periodic lattice structure around the axis, that is, $d = \text{gcd}(n, m)$ is not unity; and (2) the electrons in the low energy bands must be rotating around the axis.

In this paper, we did not consider the effect of Coulomb interactions among conducting electrons on persistent currents because this is not well understood¹⁰⁾ even for standard one-dimensional Aharonov-Bohm rings. However, there are several indications. For instance, experimentally, Chandrasekhar et al.⁹⁾ measured the magnetization of single, isolated Au loops and observed that the amplitude of the persistent currents was close to the estimated value based on theories of non-interaction. Theoretically, it is shown that for a one-dimensional model derived from the tight-binding Hamiltonian (Eq.9), the long-range part of the Coulomb interaction is ineffective, indicating that persistent currents *persist* even in the presence of external charges (Sasaki in Ref.13). Although our argument is based mainly on the kinematics, it is possible that interactions might invalidate our results.

In addition to Coulomb interactions, the Hamiltonian is expected to be modified by several factors. The surface curvature and bending of the tube is known to affect the location of the Fermi points.¹⁶⁾ Furthermore, the Euler theorem for polyhedra permits pentagon-heptagon pairs in nanotori, and a pentagon (or a heptagon) can mix the wave functions at two Fermi points¹⁷⁾ so that the persistent current is thought to be affected by their presence. This warrants future work concerning the effects of dynamical detail (surface curvature and so on) on persistent current. However, notice that the essential physics presented in this paper can be applied to persistent currents in tubule structures based not only on carbon but on other materials as well.¹⁸⁾

§7. Conclusion

The kinematics of π -electrons in carbon nanotori have been clarified and used to examine persistent currents. We have shown that persistent currents in twisted nanotori exhibit a characteristic different from that of conventional one-dimensional materials due to the fact that conducting electrons near the Fermi level are rotating around the axis. The results clearly show that the lattice structure itself allows new phenomena in the persistent currents.

We can now answer the question “How does a nanotube differ from conventional one-dimensional material, such as a chain of atoms?” posed in Section 1. The difference is that conducting electrons near the Fermi level have a degree of rotation around the nanotube tubule axis, and nanotube characteristics can be determined from the persistent currents in the nanotori.

Acknowledgments

K. S. is grateful to Dr. Y. Sumino for his continuous encouragement and outstanding instruction during the preparation of this paper. He also wishes to thank Prof. Z.F. Ezawa, Prof. K. Hikasa, Prof. N. Toyoda, and Prof. Y. Kuramoto. He would like to acknowledge the members of the High Energy Theory Group at Tohoku University, including Prof. S. Watamura, Prof. T. Moroi, Dr. M. Hotta, and Dr. H. Ishikawa. This work is supported by a fellowship of the 21st Century COE Program of the International Center of Research and Education for Materials

of Tohoku University.

References

- 1) S. Iijima, *Nature* **354** (1991), 56.
- 2) R. Saito, G. Dresselhaus, and M.S. Dresselhaus, *Physical Properties of Carbon Nanotubes*, (Imperial College Press, London, 1998).
- 3) J.W. Mintmire, B.I. Dunlap, and C.T. White, *Phys. Rev. Lett.* **68** (1992), 631; N. Hamada, S.I. Sawada, and A. Oshiyama, *Phys. Rev. Lett.* **68** (1992), 1579; R. Saito, M. Fujita, G. Dresselhaus, and M.S. Dresselhaus, *Appl. Phys. Lett.* **60** (1992), 2204.
- 4) J.W.G. Wildöer, L.C. Venema, A.G. Rinzler, R.E. Smalley, and C. Dekker, *Nature* **391** (1998), 59; T.W. Odom, J. Huang, P. Kim, and C.M. Lieber, *Nature* **391** (1998), 62.
- 5) C. Kane, L. Balents, and M.P.A. Fisher, *Phys. Rev. Lett.* **79** (1997), 5086; R. Egger and A.O. Gogolin, *Eur. Phys. J. B* **3** (1998), 281; H. Yoshioka and A.A. Odintsov, *Phys. Rev. Lett.* **82** (1999), 374.
- 6) M. Bockrath, D.H. Cobden, J. Lu, A.G. Rinzler, R.E. Smalley, L. Balents, and P.L. McEuen, *Nature* **397** (1999), 598; H.W.Ch. Postma, T. Teepen, Z. Yao, M. Grifoni, and C. Dekker, *Science* **293** (2001), 76.
- 7) J. Liu, H. Dai, J.H. Hafner, D.T. Colbert, R.E. Smalley, S.J. Tans, and C. Dekker, *Nature* **385** (1997), 780.
- 8) M. Büttiker, Y. Imry, and R. Landauer, *Phys. Lett. A* **96** (1983), 365; R. Landauer and M. Büttiker, *Phys. Rev. Lett.* **54** (1985), 2049.
- 9) L.P. Lévy, G. Dolan, J. Dunsmuir, and H. Bouchiat, *Phys. Rev. Lett.* **64** (1990), 2074; V. Chandrasekhar, R.A. Webb, M.J. Brady, M.B. Ketchen, W.J. Gallagher, and A. Klein-sasser, *Phys. Rev. Lett.* **67** (1991), 3578; D. Mailly, C. Chapelier, and A. Benoit, *Phys. Rev. Lett.* **70** (1993), 2020.
- 10) Y. Imry, *Introduction to Mesoscopic Physics*, (Oxford University Press, New York, 1997).
- 11) M.F. Lin and D.S. Chuu, *Phys. Rev. B* **57** (1998), 6731; M. Margańska and M. Szopa, *Acta Phys. Pol. B* **32** (2001), 427.
- 12) A. Ceulemans, L.F. Chibotaru, S.A. Bovin, and P.W. Fowler, *J. Chem. Phys.* **112** (2000), 4271.
- 13) M.F. Lin, R.B. Chen, and F.L. Shyu, *Solid State Comm.* **107** (1998), 227; S. Latil, S. Roche, and A. Rubio, *Phys. Rev. B* **67** (2003), 165420; A.A. Odintsov, W. Smit, and H. Yoshioka, *Europhys. Lett.* **45** (5) (1999), 598; K. Sasaki, *Phys. Rev. B* **65** (2002), 155429.
- 14) R. Martel, H.R. Shea, and P. Avouris, *Nature* **398** (1999), 299; *J. Phys. Chem. B* **103** (1999), 7551; M. Ahlskog, E. Seynaeve, R.J.M. Vullers, C. Van Haesendonck, A. Fonseca, K. Hernadi, J.N. Nagy, *Chem. Phys. Lett.* **300** (1999), 202.
- 15) A similar gauge field (commonly known as *geometry-induced gauge*) was obtained by S. Takagi and T. Tanzawa, *Prog. Theor. Phys.* **87** (1992), 561.
- 16) C.L. Kane and E.J. Mele, *Phys. Rev. Lett.* **78**, 1932 (1997); M. Ouyang, J. Huang, C.L. Cheung, and C.M. Lieber, *Science* **292** (2001), 27.
- 17) J. González, F. Guinea, and M.A. Vozmediano, *Phys. Rev. Lett.* **69** (1992), 172, *Nucl. Phys. B* **406** (1993), 771; H. Matsumura and T. Ando, *J. Phys. Soc. Jpn.* **67** (1998), 3542.
- 18) K. Sasaki, Y. Kawazoe, and R. Saito, arXiv:cond-mat/0401597.